Human Molecular Genetics, 2014, Vol. 23, No. 12 **3189–3199**
doi:10.1093/hmg/ddu029
Advance Access published on January 25, 2014

Partial restoration of cardiac function with ΔPDZ nNOS in aged mdx model of Duchenne cardiomyopathy

Yi Lai*, Junling Zhao, Yongping Yue, Nalinda B. Wasala and Dongsheng Duan*

Department of Molecular Microbiology and Immunology, University of Missouri-Columbia, Columbia, MO 65212, USA

Received December 6, 2013; Revised December 6, 2013; Accepted January 20, 2014

Transgenic gene deletion/over-expression studies have established the cardioprotective role of neuronal nitric oxide synthase (nNOS). However, it remains unclear whether nNOS-mediated heart protection can be translated to gene therapy. In this study, we generated an adeno-associated virus (AAV) nNOS vector and tested its therapeutic efficacy in the aged mdx model of Duchenne cardiomyopathy. A PDZ domain-deleted nNOS gene (ΔPDZ nNOS) was packaged into tyrosine mutant AAV-9 and delivered to the heart of ∼14-month-old female mdx mice, a phenotypic model of Duchenne cardiomyopathy. Seven months later, we observed robust nNOS expression in the myocardium. Supra-physiological ΔPDZ nNOS expression significantly reduced myocardial fibrosis, inflammation and apoptosis. Importantly, electrocardiography and left ventricular hemodynamics were significantly improved in treated mice. Additional studies revealed increased phosphorylation of phospholamban and p70S6K. Collectively, we have demonstrated the therapeutic efficacy of the AAV ΔPDZ nNOS vector in a symptomatic Duchenne cardiomyopathy model. Our results suggest that the cardioprotective role of ΔPDZ nNOS is likely through reduced apoptosis, enhanced phospholamban phosphorylation and improved Akt/mTOR/p70S6K signaling. Our study has opened the door to treat Duchenne cardiomyopathy with ΔPDZ nNOS gene transfer.

INTRODUCTION

Neuronal nitric oxide synthase (nNOS) is a calcium/calmodulin-regulated enzyme, which catalyzes the production of the signaling molecule nitric oxide (NO) from L-arginine. Although nNOS is originally discovered and highly enriched in neuronal tissues, nNOS is also expressed in the sarcoplasmic reticulum and mitochondria in the heart (1). Recent studies suggest that nNOS is a pivotal regulator of myocardial contraction (1). Specifically, nNOS-derived NO can modulate calcium cycling and redox equilibrium of the heart by promoting phospholamban phosphorylation and inhibiting xanthine oxidase (2–7). In response to the stress (such as heart failure), nNOS expression and activity are significantly elevated in the heart suggesting that nNOS may play a protective and/or adaptive role (8–12). The concept that nNOS upregulation may represent a promising therapeutic modality is further advanced by a series of transgenic studies. In these experiments, investigators found that transgenic overexpression of nNOS can effectively ameliorate heart failure caused by myocardial infarction, pressure overload or dystrophin deficiency (13–15). Despite encouraging genetic evidence, therapeutic myocardial nNOS gene transfer has never been tested.

Duchenne cardiomyopathy is a lethal inherited heart disease caused by dystrophin deficiency. While restoring dystrophin expression is the ultimate goal, attempts in this direction have been hampered by the gigantic size of the dystrophin gene and immune rejection to newly introduced dystrophin (16). Therapeutic transfer of endogenous cardioprotective genes offers an alternative approach to treat Duchenne cardiomyopathy (17,18).

Adeno-associated virus (AAV) is a dependent parvovirus. It has been successfully used in many clinical trials (19). Among various AAV serotypes, AAV-9 is especially potent for heart gene transfer in rodents (20). Tyrosine-mutated AAV has shown even higher transduction efficiency (21). In light of the superior myocardial transduction property of AAV-9 and

*To whom correspondence should be addressed at: M610, Department of Molecular Microbiology and Immunology, School of Medicine, University of Missouri, One Hospital Drive, Columbia, MO 65212, USA. Tel: +1 5738846685; Fax: +1 5738824287; Email: laiy@missouri.edu (Y.L.); M610G, Department of Molecular Microbiology and Immunology, School of Medicine, University of Missouri, One Hospital Drive, Columbia, MO 65212, USA. Tel: +1 5738849584; Fax: +1 5738824287; Email: duand@missouri.edu (D.D.)

the therapeutic potential of nNOS overexpression, we decided to test the hypothesis that tyrosine mutant AAV-9-mediated nNOS gene therapy can ameliorate dilated cardiomyopathy in aged female dystrophin-null mdx mice, a symptomatic Duchenne cardiomyopathy model (22,23).

Unlike other viral gene transfer vectors (such as adenovirus and retrovirus), AAV has a fairly small carrying capacity. Genomes that are >5-kb are poorly packaged (24). Unfortunately, the size of the full-length nNOS expression cassette exceeds this 5-kb limit. To package nNOS into an AAV vector, part of nNOS coding sequence has to be removed.

The active form of nNOS is a dimer. Each monomer is composed of a calmodulin-binding site and three structural domains including the oxygenase, reductase and PDZ domain (Supplementary Material, Fig. S1) (25). The calmodulin-binding site recruits calmodulin. Calcium binding to calmodulin leads to the dimerization of two monomers into a functional enzyme. The oxygenase domain contains the L-arginine, heme and tetrahydrobiopterin-binding sites, whereas the reductase domain contains the flavin mononucleotide, flavin adenine dinucleotide and nicotinamide adenine dinucleotide phosphate-binding sites. The oxygenase and reductase domains are essential for the enzymatic activity.

The PDZ domain of nNOS consists of the N-terminal 226 amino acid residues. This domain is thought to not contribute to NO production but rather responsible for mediating protein–protein interactions between nNOS and other cellular proteins. In support of this notion, Brenman *et al.* found that the enzymatic activity of a PDZ domain-deleted nNOS mutant (ΔPDZ nNOS) is identical to that of the full-length protein (26). Since our goal is to determine myocardial protection by nNOS-derived NO, we constructed our AAV vector with the ΔPDZ nNOS mutant (Supplementary Material, Fig. S1). To limit untoward expression in non-muscle tissues, we also used a synthetic muscle-specific promoter (SPc5-12) (27). Gene transfer resulted in robust nNOS expression in the whole heart. Importantly, ΔPDZ nNOS therapy significantly mitigated heart pathology and improved heart function in aged mdx mice.

RESULTS

Robust expression of ΔPDZ nNOS in the heart of aged mdx mice

To achieve efficient viral packaging, we intentionally removed the PDZ domain and generated the ΔPDZ nNOS AAV vector (Supplementary Material, Fig. S1). The ΔPDZ nNOS construct was then packaged in tyrosine mutant AAV-9 vector and delivered to the heart of ∼14-month-old (13.6 ± 0.7) female mdx mice at the dose of 1×10^{13} viral genome particles/mouse. Seven months later, we examined transduction efficiency.

Nominal nNOS activity was detected by *in situ* staining in the hearts of BL10 and mdx mice (Fig. 1A). In sharp contrast, AAV-treated mdx heart showed widespread myocardial nNOS activity (Fig. 1A). The high-power image revealed homogenous nNOS activity in transduced cardiomyocytes (Fig. 1A, inset). To further clarify the subcellular location of ΔPDZ nNOS, we performed double immunofluorescence staining in serial tissue sections (Supplementary Material, Fig. S2). Using the flag antibody and an nNOS C-terminus antibody, we observed evenly distributed ΔPDZ nNOS throughout the cytosol (Supplementary Material, Fig. S2). Consistent with this finding, co-localization study with antibodies against α-actinin (a Z disk marker), phospholamban (a sarcoplasmic reticulum marker) and cytochrome *C* (a mitochondria marker) did not show an enrichment of ΔPDZ nNOS in these subcellular compartments (Supplementary Material, Fig. S2).

Immunoblot confirmed robust expression of vector-derived ΔPDZ nNOS in AAV-injected mdx heart (Fig. 1B). Additional studies showed that ΔPDZ nNOS expression did not alter the expression of utrophin, endothelial NOS (eNOS), inducible NOS (iNOS) and endogenous nNOS in the heart of aged mdx mice (Fig. 1C).

ΔPDZ nNOS gene therapy ameliorated dystrophic cardiomyopathy

Several pathologic electrocardiography (ECG) changes (such as sinus tachycardia, PR interval reduction, QTc elongation and elevated cardiomyopathy index) were normalized in treated mice (Fig. 2A, Supplementary Material, Table S1). On cardiac catheter assay, we did not see a significant change in end systolic/diastolic volume in treated mice (Fig. 2B, Supplementary Material, Table S2). However, the kinetics of ventricular pressure change during myocardial contraction and relaxation were significantly improved by ΔPDZ nNOS therapy (Fig. 2B). The maximal systolic pressure and isovolumic relaxation constant (tau) also showed a trend towards normalization in treated mice (Fig. 2B). Notably, indices of overall heart function (ejection fraction, stroke volume and cardiac output) were significantly increased following AAV therapy (Fig. 2B, Supplementary Material, Table S2).

Consistent with electrophysiologic and hemodynamic improvement seen in functional assays (Fig. 2), histopathology studies revealed significant reduction of myocardial fibrosis and neutrophil infiltration (Fig. 3A). AAV therapy also significantly reduced apoptosis in dystrophic heart as measured by terminal deoxynucleotidyl transferase dUTP nick end labeling (TUNEL) and caspase-3 immunostaining (Fig. 3B). Nonetheless, supra-physiological ΔPDZ nNOS expression did not alter myocardial vascularization (Fig. 4). The numbers of arterioles and capillaries were similar among three experimental groups (Fig. 4).

Therapeutic ΔPDZ nNOS expression modulates phosphorylation of phospholamban and p70S6K

Lack of dystrophin significantly reduced phosphorylation of phospholamban in aged mdx heart. Forced ΔPDZ nNOS expression partially restored phospholamban phosphorylation (Fig. 5). No significant difference was noticed among experimental groups for other calcium regulating proteins including SERCA2a, ryanodine receptor 2, calsequestrin and Na^+/K^+ ATPase (Supplementary Material, Fig. S3). A trend of increased p38 phophorylation was seen in untreated mdx heart, but not in AAV-treated mdx heart (Fig. 5). Akt and phosphorylated Akt did not show significant differences among normal, mdx and treated mdx hearts (Fig. 5). Phosphorylated mTOR appeared diminished in mdx heart irrespective of AAV therapy (Fig. 5). Notably, ΔPDZ nNOS overexpression significantly increased the level of phosphorylated p70S6K in mdx heart (Fig. 5).

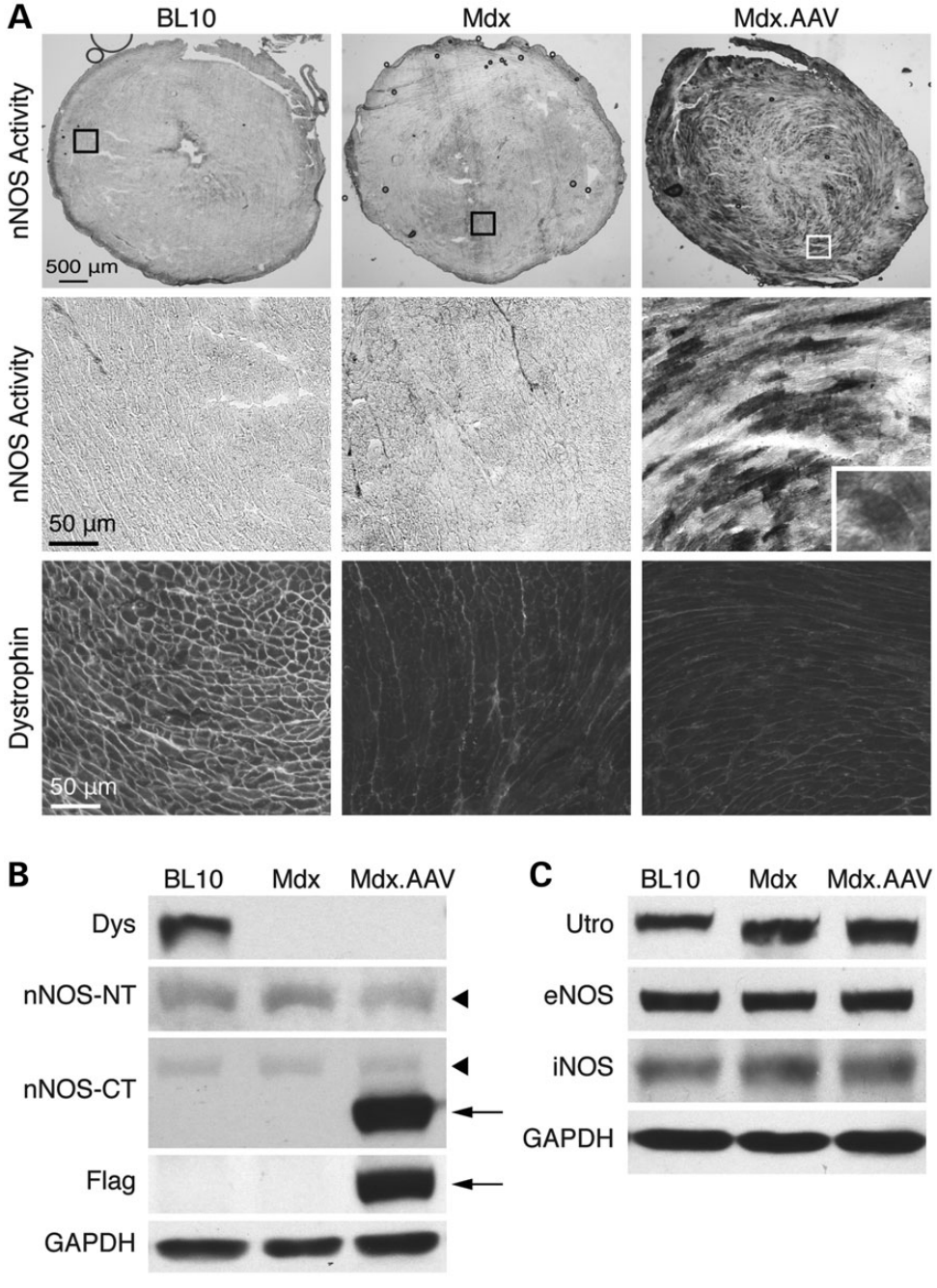

Figure 1. Robust myocardial expression of ΔPDZ nNOS. Aged female mdx mice were infected with a tyrosine mutant AAV-9 vector expressing the ΔPDZ nNOS gene. Animals were euthanized 7 months later for immunostaining and western blot study. (**A**) Dystrophin immunostaining and nNOS activity staining. Top panel: representative photomicrographs of nNOS activity staining of the full-view heart section. Middle and bottom panels: representative photomicrographs of nNOS activity staining and dystrophin immunostaining of the respective boxed areas in the top panel. Inset: a high-power image showing even distribution of ΔPDZ nNOS in a cardiomyocyte. (**B**) Immunoblot for dystrophin (Dys), nNOS and Flag. nNOS was detected with an nNOS N-terminal-specific antibody (nNOS-NT) and an nNOS C-terminal-specific antibody (nNOS-CT). Arrowhead: endogenous nNOS; arrow: ΔPDZ nNOS. (**C**) Immunoblot for utrophin (utro), eNOS and iNOS. GAPDH serves as the loading control for immunoblot.

DISCUSSION

In this study, we showed that gene therapy with a PDZ domain truncated nNOS gene significantly ameliorated heart disease in a symptomatic Duchenne cardiomyopathy model (Figs 2 and 3). We further showed that the benefit of ΔPDZ nNOS might represent a collective effect of reduced apoptosis, enhanced phospholamban phosphorylation and improved p70S6K signaling (Figs 3 and 5).

In skeletal muscle, nNOS is localized at the sarcolemma by a dystrophin-mediated mechanism (28,29). Loss of dystrophin detargets nNOS away from the sarcolemma and reduces total cellular nNOS level in skeletal muscle. Loss of

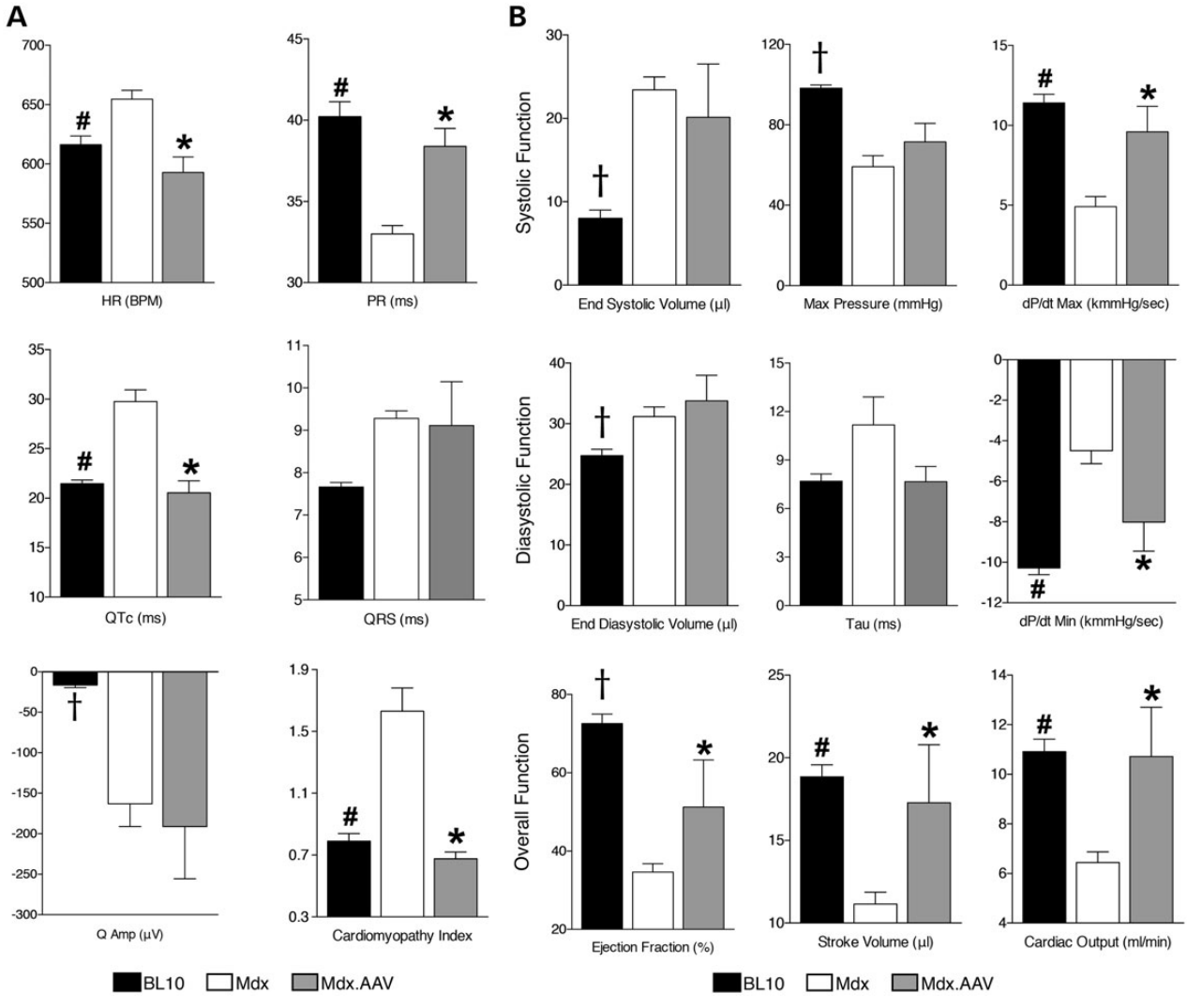

Figure 2. AAV-mediated ΔPDZ nNOS expression improves cardiac function in aged mdx model. (**A**) ECG results. $N = 11$, 12 and 9 for BL10, untreated and treated mdx, respectively. (**B**) Left ventricular hemodynamic results. $N = 16$, 13 and 5 for BL10, untreated and treated mdx, respectively. Asterisk: treated mdx is significantly different from that of untreated mdx; pound sign: BL10 is significantly different from that of untreated mdx; cross: significantly different from other two groups.

membrane-associated nNOS is an important pathogenic mechanism for skeletal muscle disease in Duchenne muscular dystrophy. In contrast to skeletal muscle, nNOS is primarily localized in the sarcoplasmic reticulum and mitochondria in the heart (30,31). Further, dystrophin deficiency did not alter the myocardial nNOS level (Fig. 1B) (15). Currently, little is known about the role nNOS plays in the pathogenesis of Duchenne cardiomyopathy.

Cardiac consequences of nNOS deficiency and overexpression have been extensively investigated using loss- and gain-of-function transgenic models, respectively (1). Although many issues remain to be resolved, the consensuses are (i) absence of nNOS decreases phospholamban phosphorylation and (ii) supra-physiological nNOS expression protects the heart in various disease models (13–15).

To determine whether the perceived cardioprotective function of nNOS can be capitalized for gene therapy, we generated an AAV nNOS vector. AAV is one of the most promising gene transfer vehicles for clinical translation (19). However, AAV has a small packaging capacity. It is insufficient for delivering the full-length nNOS gene expression cassette (24). To generate an AAV nNOS vector, we removed the non-catalytic PDZ domain from the nNOS gene (Supplementary Material, Fig. S1). The PDZ domain truncated nNOS gene was then delivered to the heart of old female mdx mice using tyrosine mutant AAV-9.

To evaluate gene transfer efficiency, we performed *in situ* nNOS activity assay. Previous biochemistry studies suggest that nNOS expression is localized in the sarcolemma and mitochondria in normal heart (30,31). Intriguingly, minimal nNOS activity was detected in the heart of control BL10 mice by *in situ* staining (Fig. 1A). Nevertheless, we observed robust widespread nNOS activity in the cardiomyocytes of the treated mdx heart (Fig. 1A).

To study physiological and histologic impact of ΔPDZ nNOS overexpression, we compared ECG, left ventricular

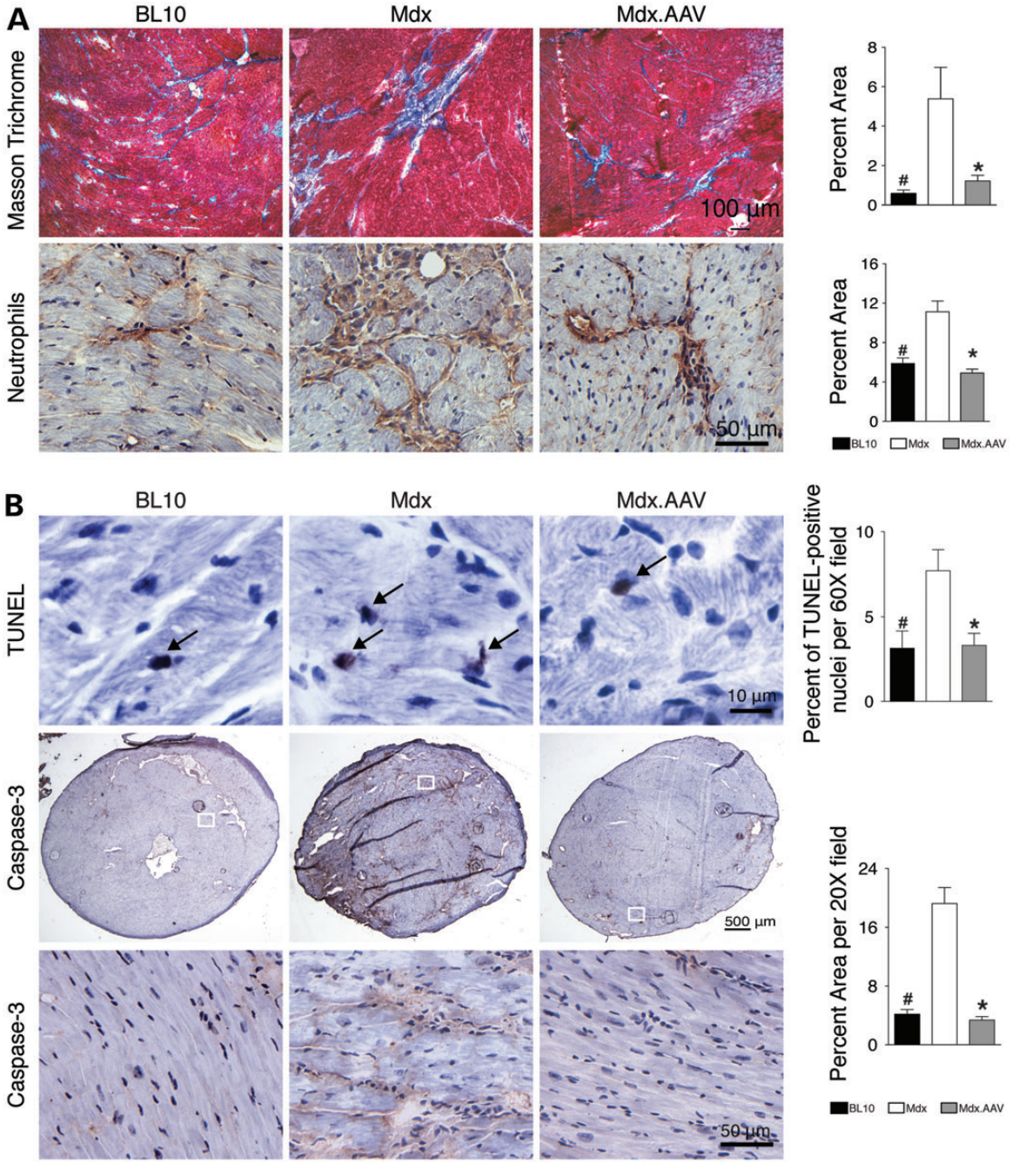

Figure 3. ΔPDZ nNOS expression reduces myocardial fibrosis, inflammation and apoptosis. (**A**) Representative photomicrographs of Masson trichrome staining (for fibrosis) and neutrophil immunohistochemical staining. Bar graphs show quantification results. $N = 3, 4$ and 6 for BL10, untreated and treated mdx, respectively. (**B**) Representative photomicrographs of TUNEL assay and Caspase-3 immunostaining. Bar graphs represent quantification results. $N = 3, 4$ and 6 for BL10, untreated and treated mdx, respectively, in TUNEL assay; $N = 3, 4$ and 6 for BL10, untreated and treated mdx, respectively, in Caspase-3 immunostaining. Asterisk: treated mdx is significantly different from that of untreated mdx; Pound sign: BL10 is significantly different from that of untreated mdx.

hemodynamics and heart pathology among normal, untreated and AAV-treated mdx mice (Figs 2 and 3). Consistent with our previous reports (23,32–34), characteristic signs of Duchenne cardiomyopathy (such as tachycardia, PR interval diminution, chamber dilation, cardiac output reduction, fibrosis and inflammation) were observed in untreated mdx mice (Figs 2 and 3). AAV-mediated ΔPDZ nNOS therapy resulted in significant improvement in most, but not all disease markers (Figs 2 and 3).

To better understand cellular mechanisms underlying our observation, we quantified apoptosis and vascularization (Figs 3 and 4). Apoptosis has been considered as a mechanism of myofiber death in DMD (35,36). Indeed, we observed significantly more

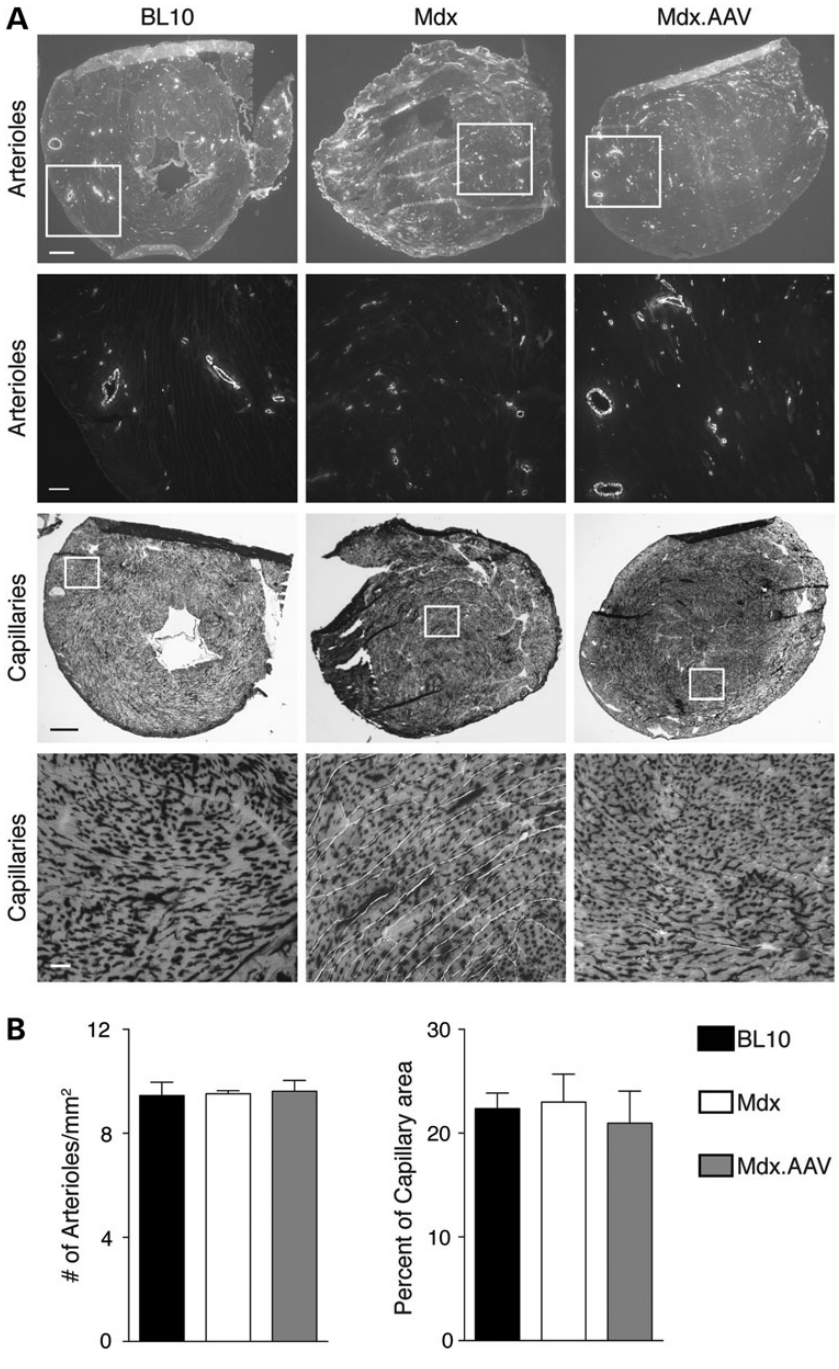

Figure 4. Supra-physiological ΔPDZ nNOS expression does not alter the density of the vasculature in the heart. Arterioles and capillaries in the heart were evaluated by anti-α smooth muscle actin immunostaining and capillaries staining, respectively. (**A**) Representative photomicrographs of arterioles immunostaining (scale bar: top panel 500 μm; bottom panel 100 μm) and capillaries staining (scale bar: top panel 500 μm; bottom panel 50 μm). (**B**) Quantification of staining results. $N = 4, 3$ and 6 for BL10, untreated and treated mdx, respectively, in arterioles' staining; $N = 4, 4$ and 5 for BL10, untreated and treated mdx, respectively, in capillaries staining.

TUNEL-positive myonuclei and a larger area of caspase-3 positive staining in the heart of untreated mdx mice (Fig. 3B). These apoptotic biomarkers were normalized following ΔPDZ nNOS therapy suggesting that decreased cardiomyocyte death may have contributed to the reduction of myocardial fibrosis (Fig. 3A). nNOS has been recognized as a critical regulator of vascular hemostasis (37). A recent study further correlated nNOS expression with exercise-induced angiogenesis in human skeletal muscle (38). To determine whether increased vascularization underlay myocardial protection of ΔPDZ nNOS therapy, we quantified the density of arterioles and capillaries in the heart of normal, untreated and AAV-treated mdx heart (Fig. 4). No difference was found among experimental groups (Fig. 4). Our results suggest that vascularization is not altered in the heart of aged mdx mice. Further, ΔPDZ nNOS overexpression has minimal impact on myocardial angiogenesis.

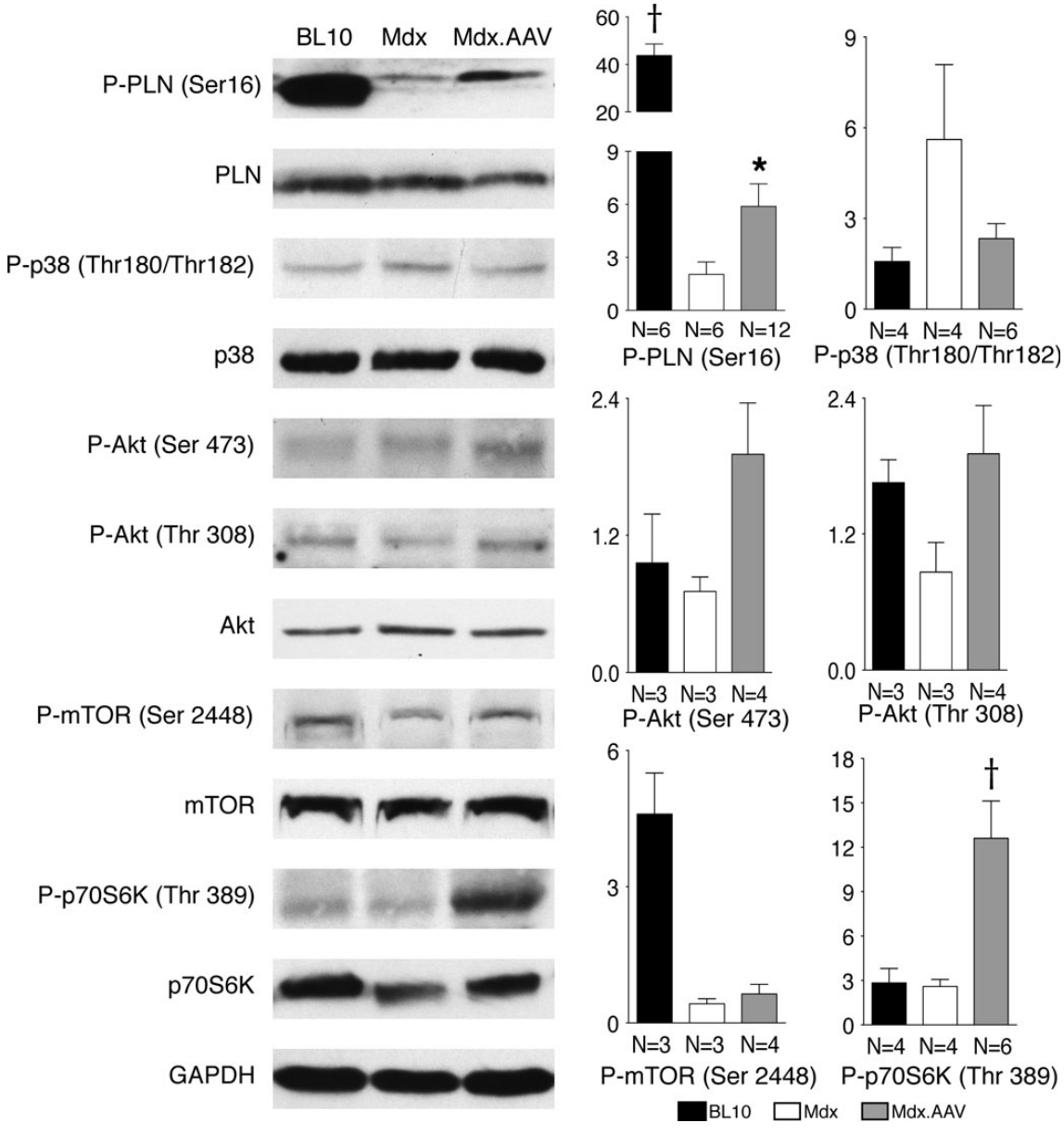

Figure 5. Immunoblot examination of phospholamban (PLN), p38 and the Akt/mTOR/p70S6K pathway. Left panels: representative immunoblot for each indicated protein and their phosphorylated form. Right panels: densitometry quantification results. The sample size is marked in bar graphs for each group. Asterisk: treated mdx is significantly different from that of untreated mdx; cross: significantly different from other two groups.

Enhanced phospholamban phosphorylation and reduced oxidative stress have been proposed as the protective mechanisms in heart-specific nNOS transgenic mice (13,14). Here, we focused on phospholamban. Phospholamban is a reversible inhibitory calcium pump regulator. Unphosphorylated phospholamban binds to sarcoplasmic reticulum calcium ATPase 2a (SERCA 2a) and inhibits SERCA2a activity. Upon phosphorylation, phospholamban disassociates from SERCA2a. This conformational change activates SERCA2a. Consequently, calcium recycling is improved and myocardial contractility is enhanced (39). To determine whether ΔPDZ nNOS overexpression alters the molecular status of phospholamban, we quantified the levels of total and phosphorylated phospholamban (Fig. 5). No significant difference was noted in total phospholamban. However, phosphorylated phospholamban was significantly reduced in the mdx heart. AAV nNOS therapy significantly enhanced phospholamban phosphorylation in treated mdx heart (Fig. 5). Since aberrant cytosolic calcium elevation is a pathogenic feature of dystrophin-null myocytes (40), we also examined the levels of several other calcium regulating proteins including SERCA2a, ryanodine receptor 2, calsequestrin and Na+/K+ ATPase (Supplementary Material, Fig. S3). Nominal differences were noted in these proteins among three experimental groups. Our results suggest that improved phospholamban phosphorylation may at least in part explain the observed myocardial function improvement (Figs 2 and 5) (13,41).

To gain more mechanistic insight, we also studied p38 stress kinase and the Akt/mTOR/p70S6K pathway (Fig. 5). This

pathway has been implicated in myocardial protection (42,43). We did not see statistically significant differences in p38 and phosphorylated p38, Akt and phosphorylated Akt, mTOR and phosphorylated mTOR and p70S6K among experimental groups (Fig. 5). However, compared with that of untreated mdx, threonine 389 phosphorylated p70S6K was significantly elevated in AAV-treated mice (Fig. 5). The p70S6K is a critical regulator for protein synthesis and cell proliferation (44). Over-expression of p70S6K stimulates protein synthesis in cardiomyocytes (45,46). Knockout of all p70S6K isoforms results in perinatal death and dilated cardiomyopathy (45,47). Our results are consistent with the literature and suggesting that activation of p70S6K through the pro-survival Akt/mTOR/p70S6K pathway may have contributed to the therapeutic effect of ΔPDZ nNOS.

In this study, we intentionally deleted the PDZ domain. This domain is thought to guide subcellular localization but does not directly participate in NO synthesis. Since subcellular localization may greatly influence molecular consequences and phenotypic outcome of nNOS over-expression (13,14), it will be interesting to determine how the truncation of the PDZ domain affects nNOS localization. In heart-specific full-length nNOS transgenic mice, over-expressed nNOS is enriched at the sarcolemma or mitochondria (13,14). In sharp contrast, we did not see evidence of subcellular aggregation of ΔPDZ nNOS (Fig. 1A; Supplementary Material, Fig. S2). In fact, it is extensively dispersed throughout the cytosol (Fig. 1A; Supplementary Material, Fig. S2). Our results are consistent with the perceived role of the PDZ domain for molecular targeting. In light of the physiological/histological improvement seen in AAV-treated mdx heart, it appears that the enzymatic activity of nNOS *per se* might be sufficient to ameliorate dystrophic cardiomyopathy. Future studies are needed to determine whether subcellular targeting can further enhance nNOS therapy and more importantly whether our approach can be used to treat other heart diseases.

MATERIALS AND METHODS

Animals

All animal experiments were approved by the Animal Care and Use Committee of the University of Missouri and were performed in accordance with NIH guidelines. Dystrophin-null female mdx (C57BL/10ScSn-*Dmd*^{mdx}/J) mice and wild-type C57Bl/10 (BL10) mice were originally purchased from The Jackson Laboratory (Bar Harbor, ME, USA). Experimental mice were generated by in house breeding. Mice were housed in a specific-pathogen-free animal facility.

Recombinant AAV.ΔPDZ nNOS vector

The first 226 residues consist of the PDZ domain in nNOS. These 226 residues are removed in ΔPDZ nNOS (Supplementary Material, Fig. S1A). The rat nNOS-α cDNA (a gift from David Bredt, UCSF, San Francisco, CA, USA) was used as the template to generate the ΔPDZ nNOS gene by PCR (26). The forward primer was 5′-gcgcatgcat*cgccacc*ATGGACTACAAGGACG ACGATGACAAGgagatgaaagacacaggaatccaggtggacagagacct-cgatgg-3′ (italic: Kozak sequence; uppercase: Flag tag). The reverse primer was 5′-gctagcttaggagctgaaaacctcatctgcgtctttt ttgctctcttcg-3′. To distinguish ΔPDZ nNOS from endogenous nNOS, we fused the Flag tag at the 5′-end of ΔPDZ nNOS gene (Supplementary Material, Fig. S1B). The muscle-specific promoter SPc5-12 was used to drive Flag-ΔPDZ nNOS expression (Supplementary Material, Fig. S1B) (27). We first generated an intermediate packaging plasmid called AAV.SPc5-12 (pYL276). The final AAV packaging plasmid pcis.SPc5-12.Flag-ΔPDZ nNOS (pYL349) was generated by cloning the Flag-ΔPDZ nNOS gene into the AAV.SPc5-12 plasmid. The authenticity of the Flag-ΔPDZ nNOS gene was confirmed by sequencing. Recombinant vector was packaged into AAV-9 Y731F tyrosine mutant (48). AAV was purified according to our previously published method (28). The viral titer was quantified by real-time PCR. The forward primer was 5′-gagaag gaacagtcccctacctcgggg-3′. The reverse primer was 5′-ggcagcat gatcgagcccatg-3′.

AAV injection and animal experiment overview

1×10^{13} viral genome particles per mouse of AAV vectors were injected to ∼14-month-old female mdx mice via the tail vein. ECG and left ventricular hemodynamic catheter assay were carried out 7 months after injection. During the 7-month observation window, none of the AAV-injected mdx mice died. Age- and sex-matched BL10 and untreated mdx mice were used as controls.

Twelve-lead ECG analysis

The non-invasive 12-lead ECG assay was performed according to our published method (34,49). Mice first received isoflurane anesthesia and then were placed on a heating pad to keep body temperature constant at 37°C. Cardiac electric activity was collected and recorded by inserting needle electrodes into limbs and the chest wall. Switching the lead was achieved by changing the position of the chest lead. Total 12-lead ECG signal was recorded by the model MLA0112S PowerLab system connected with a single-channel bioamplifier (ML132, ADInstruments, Colorado Springs, CO, USA). The calculation of the Q wave amplitude was based on the ECG results from lead I and aVL while the rest of ECG parameters was examined according to the ECG results from lead II.

Catheter-mediated left ventricle hemodynamic function assay

Hemodynamic function was evaluated according to our published protocol (32,34). Mice were anesthetized with isoflurane and put on the heating pad to maintain body temperature at 37°C. A microtip pressure–volume (PV) catheter (SPR-839, Millar Instrument, Houston, TX, USA) was passed through the right carotid artery into the left ventricle. Hemodynamic data were gathered with the Millar Aria-1 PV conductance system and examined with the PVAN software (Millar Instrument).

Histology

Histological staining was performed on 8 μm cryo-sections. nNOS activity assay was performed using our published protocol (28,29). Dystrophin expression was examined by immunofluorescence staining with the Dys-2 antibody (1:20, Novocastra). Neutrophils were detected by immunohistochemical staining with the rat anti-mouse Ly-6G antibody (1:8000, CADO48A, VRMD). Arterioles were revealed by anti-α smooth muscle actin immunofluorescence staining (1:2000, A2547, Sigma). Caspase-3 was identified by immunohistochemical staining with anti-caspase 3 antibody (1:200, 559565, BD Biosciences). Cardiac fibrosis was investigated with Masson Trichrome staining as our published methods (32). TUNEL assay was performed according to manufactures' manual (Dead-End™ Colorimetric TUNEL system, G7360, Promega) and nuclei were counterstained with hematoxylin. The capillary staining was carried out as previously published (50).

For double immunofluorescence staining on serial sections, nNOS was detected with an antibody specific for the nNOS C-terminus (1:1000, N7280, Sigma). Other antibodies are used to recognize the flag tag (1:100, F1804, Sigma), α-actinin (1:100, A-7811, Sigma), phospholamban (1:200, A010-14, Badrilla) and cytochrome *C* (1:400, 556432, BD Biosciences). The myonuclei were stained with DAPI.

Quantification of cardiac fibrosis, inflammation and apoptosis (Caspase-3) was carried out as previously published methods (51). Briefly, the serial sections were stained as described above and positively stained area was assessed from digitized images using the ImageJ software (http://rsb.info.nih.gov/ij/). Positively stained area was separated from non-stained area by color threshold as the published protocols (52). The percentage of the positive stained area was calculated.

TUNEL-positive nuclei were quantified with the counting tool in ImageJ. The percentage of TUNEL-positive nuclei was calculated by dividing the number of positively stained nuclei with the number of total nuclei in the same field.

Immunoblot

Heart tissue samples were homogenized in the homogenization buffer containing 10% sodium dodecyl sulfate (SDS), 5 mM ethylenediaminetetraacetic acid, 62.5 mM Tris–HCl (pH 6.8), plus 1% cocktail proteinase inhibitor (Catalog no.: 118361 53001, Roche Applied Science) and 1% phosphatase inhibitor cocktail A (sc-45044, Santa Cruz Biotechnology). Proteins were resolved in 6–10% SDS–polyacrylamide gel and the target proteins were detected by the antibodies listed in Supplementary Material, Table S3. Each immunoblot was repeated at least three times and the representative image was presented. Signal intensity was quantified with the software Quantity One (Ver 4.6.2, Bio-Rad, Hercules, CA, USA) as we previously published (53).

Statistical analysis

The data were analyzed with the statistical software GraphPad Prism 5.0a for Mac OS X (GraphPad Software, La Jolla, CA, USA). First, the difference among BL10, mdx and AAV-treated mdx group was compared by one-way analysis of variance test. Then the comparison between mdx and AAV-treated mdx group was done by Tukey's multiple comparisons test. The difference is regarded as significant when the *P*-value is <0.05.

SUPPLEMENTARY MATERIAL

Supplementary Material is available at *HMG* online.

ACKNOWLEDGMENT

We thank Dr Brian Bostick for technique assistance.

Conflict of Interest statement. None declared.

FUNDING

We thank the Inovio Pharmaceuticals, Inc. (Blue Bell, PA, USA) for providing the SPc5-12 promoter. This work was supported by grants from the National Institutes of Health (HL91883, D.D.), Muscular Dystrophy Association (D.D.) and Parent Project Muscular Dystrophy (D.D.).

REFERENCES

1. Zhang, Y.H. and Casadei, B. (2012) Sub-cellular targeting of constitutive NOS in health and disease. *J. Mol. Cell Cardiol.*, **52**, 341–350.
2. Sears, C.E., Bryant, S.M., Ashley, E.A., Lygate, C.A., Rakovic, S., Wallis, H.L., Neubauer, S., Terrar, D.A. and Casadei, B. (2003) Cardiac neuronal nitric oxide synthase isoform regulates myocardial contraction and calcium handling. *Circ. Res.*, **92**, e52–e59.
3. Khan, S.A., Skaf, M.W., Harrison, R.W., Lee, K., Minhas, K.M., Kumar, A., Fradley, M., Shoukas, A.A., Berkowitz, D.E. and Hare, J.M. (2003) Nitric oxide regulation of myocardial contractility and calcium cycling: independent impact of neuronal and endothelial nitric oxide synthases. *Circ. Res.*, **92**, 1322–1329.
4. Ashley, E.A., Sears, C.E., Bryant, S.M., Watkins, H.C. and Casadei, B. (2002) Cardiac nitric oxide synthase 1 regulates basal and beta-adrenergic contractility in murine ventricular myocytes. *Circulation*, **105**, 3011–3016.
5. Steppan, J., Ryoo, S., Schuleri, K.H., Gregg, C., Hasan, R.K., White, A.R., Bugaj, L.J., Khan, M., Santhanam, L., Nyhan, D. *et al.* (2006) Arginase modulates myocardial contractility by a nitric oxide synthase 1-dependent mechanism. *Proc. Natl. Acad. Sci. USA*, **103**, 4759–4764.
6. Khan, S.A., Lee, K., Minhas, K.M., Gonzalez, D.R., Raju, S.V., Tejani, A.D., Li, D., Berkowitz, D.E. and Hare, J.M. (2004) Neuronal nitric oxide synthase negatively regulates xanthine oxidoreductase inhibition of cardiac excitation-contraction coupling. *Proc. Natl. Acad. Sci. USA*, **101**, 15944–15948.
7. Kinugawa, S., Huang, H., Wang, Z., Kaminski, P.M., Wolin, M.S. and Hintze, T.H. (2005) A defect of neuronal nitric oxide synthase increases xanthine oxidase-derived superoxide anion and attenuates the control of myocardial oxygen consumption by nitric oxide derived from endothelial nitric oxide synthase. *Circ. Res.*, **96**, 355–362.
8. Dawson, D., Lygate, C.A., Zhang, M.H., Hulbert, K., Neubauer, S. and Casadei, B. (2005) nNOS gene deletion exacerbates pathological left ventricular remodeling and functional deterioration after myocardial infarction. *Circulation*, **112**, 3729–3737.
9. Damy, T., Ratajczak, P., Robidel, E., Bendall, J.K., Oliviero, P., Boczkowski, J., Ebrahimian, T., Marotte, F., Samuel, J.L. and Heymes, C. (2003) Up-regulation of cardiac nitric oxide synthase 1-derived nitric oxide after myocardial infarction in senescent rats. *FASEB J.*, **17**, 1934–1936.
10. Burger, D.E., Lu, X., Lei, M., Xiang, F.L., Hammoud, L., Jiang, M., Wang, H., Jones, D.L., Sims, S.M. and Feng, Q. (2009) Neuronal nitric oxide synthase protects against myocardial infarction-induced ventricular arrhythmia and mortality in mice. *Circulation*, **120**, 1345–1354.
11. Damy, T., Ratajczak, P., Shah, A.M., Camors, E., Marty, I., Hasenfuss, G., Marotte, F., Samuel, J.L. and Heymes, C. (2004) Increased neuronal nitric

oxide synthase-derived NO production in the failing human heart. *Lancet*, **363**, 1365–1367.
12. Bendall, J.K., Damy, T., Ratajczak, P., Loyer, X., Monceau, V., Marty, I., Milliez, P., Robidel, E., Marotte, F., Samuel, J.L. and Heymes, C. (2004) Role of myocardial neuronal nitric oxide synthase-derived nitric oxide in beta-adrenergic hyporesponsiveness after myocardial infarction-induced heart failure in rat. *Circulation*, **110**, 2368–2375.
13. Loyer, X., Gomez, A.M., Milliez, P., Fernandez-Velasco, M., Vangheluwe, P., Vinet, L., Charue, D., Vaudin, E., Zhang, W., Sainte-Marie, Y. *et al.* (2008) Cardiomyocyte overexpression of neuronal nitric oxide synthase delays transition toward heart failure in response to pressure overload by preserving calcium cycling. *Circulation*, **117**, 3187–3198.
14. Burkard, N., Williams, T., Czolbe, M., Blomer, N., Panther, F., Link, M., Fraccarollo, D., Widder, J.D., Hu, K., Han, H. *et al.* (2010) Conditional overexpression of neuronal nitric oxide synthase is cardioprotective in ischemia/reperfusion. *Circulation*, **122**, 1588–1603.
15. Wehling-Henricks, M., Jordan, M.C., Roos, K.P., Deng, B. and Tidball, J.G. (2005) Cardiomyopathy in dystrophin-deficient hearts is prevented by expression of a neuronal nitric oxide synthase transgene in the myocardium. *Hum. Mol. Genet.*, **14**, 1921–1933.
16. Duan, D. (2006) Challenges and opportunities in dystrophin-deficient cardiomyopathy gene therapy. *Hum. Mol. Genet.*, **15**, R253–R261.
17. Jessup, M., Greenberg, B., Mancini, D., Cappola, T., Pauly, D.F., Jaski, B., Yaroshinsky, A., Zsebo, K.M., Dittrich, H. and Hajjar, R.J. (2011) Calcium Upregulation by Percutaneous Administration of Gene Therapy in Cardiac Disease (CUPID): a phase 2 trial of intracoronary gene therapy of sarcoplasmic reticulum Ca2+-ATPase in patients with advanced heart failure. *Circulation*, **124**, 304–313.
18. Shin, J.H., Bostick, B., Yue, Y., Hajjar, R. and Duan, D. (2011) SERCA2a gene transfer improves electrocardiographic performance in aged mdx mice. *J. Transl. Med.*, **9**, 132.
19. Mingozzi, F. and High, K.A. (2011) Therapeutic in vivo gene transfer for genetic disease using AAV: progress and challenges. *Nat. Rev. Genet.*, **12**, 341–355.
20. Lai, Y. and Duan, D. (2012) Progress in gene therapy of dystrophic heart disease. *Gene Ther.*, **19**, 678–685.
21. Zhong, L., Li, B., Mah, C.S., Govindasamy, L., Agbandje-McKenna, M., Cooper, M., Herzog, R.W., Zolotukhin, I., Warrington, K.H.J., Weigel-Van Aken, K.A. *et al.* (2008) Next generation of adeno-associated virus 2 vectors: point mutations in tyrosines lead to high-efficiency transduction at lower doses. *Proc. Natl. Acad. Sci. USA*, **105**, 7827–7832.
22. Bostick, B., Yue, Y., Long, C., Marschalk, N., Fine, D.M., Chen, J. and Duan, D. (2009) Cardiac expression of a mini-dystrophin that normalizes skeletal muscle force only partially restores heart function in aged Mdx mice. *Mol. Ther.*, **17**, 253–261.
23. Bostick, B., Yue, Y. and Duan, D. (2010) Gender influences cardiac function in the mdx model of Duchenne cardiomyopathy. *Muscle Nerve*, **42**, 600–603.
24. Lai, Y., Yue, Y. and Duan, D. (2010) Evidence for the failure of adeno-associated virus serotype 5 to package a viral genome > or = 8.2 kb. *Mol. Ther.*, **18**, 75–79.
25. Snyder, S.H. and Ferris, C.D. (2000) Novel neurotransmitters and their neuropsychiatric relevance. *Am. J. Psychiatry*, **157**, 1738–1751.
26. Brenman, J.E., Chao, D.S., Xia, H., Aldape, K. and Bredt, D.S. (1995) Nitric oxide synthase complexed with dystrophin and absent from skeletal muscle sarcolemma in Duchenne muscular dystrophy. *Cell*, **82**, 743–752.
27. Li, X., Eastman, E.M., Schwartz, R.J. and Draghia-Akli, R. (1999) Synthetic muscle promoters: activities exceeding naturally occurring regulatory sequences. *Nat. Biotechnol.*, **17**, 241–245.
28. Lai, Y., Zhao, J., Yue, Y. and Duan, D. (2013) alpha2 and alpha3 helices of dystrophin R16 and R17 frame a microdomain in the alpha1 helix of dystrophin R17 for neuronal NOS binding. *Proc. Natl. Acad. Sci. USA*, **110**, 525–530.
29. Lai, Y., Thomas, G.D., Yue, Y., Yang, H.T., Li, D., Long, C., Judge, L., Bostick, B., Chamberlain, J.S., Terjung, R.L. and Duan, D. (2009) Dystrophins carrying spectrin-like repeats 16 and 17 anchor nNOS to the sarcolemma and enhance exercise performance in a mouse model of muscular dystrophy. *J. Clin. Invest.*, **119**, 624–635.
30. Xu, K.Y., Huso, D.L., Dawson, T.M., Bredt, D.S. and Becker, L.C. (1999) Nitric oxide synthase in cardiac sarcoplasmic reticulum. *Proc. Natl. Acad. Sci. USA*, **96**, 657–662.
31. Kanai, A.J., Pearce, L.L., Clemens, P.R., Birder, L.A., VanBibber, M.M., Choi, S.Y., de Groat, W.C. and Peterson, J. (2001) Identification of a neuronal nitric oxide synthase in isolated cardiac mitochondria using electrochemical detection. *Proc. Natl. Acad. Sci. USA*, **98**, 14126–14131.
32. Bostick, B., Yue, Y., Long, C. and Duan, D. (2008) Prevention of dystrophin-deficient cardiomyopathy in twenty-one-month-old carrier mice by mosaic dystrophin expression or complementary dystrophin/utrophin expression. *Circ. Res.*, **102**, 121–130.
33. Bostick, B., Shin, J.H., Yue, Y. and Duan, D. (2011) AAV-microdystrophin therapy improves cardiac performance in aged female mdx mice. *Mol. Ther.*, **19**, 1826–1832.
34. Bostick, B., Shin, J.H., Yue, Y., Wasala, N.B., Lai, Y. and Duan, D. (2012) AAV micro-dystrophin gene therapy alleviates stress-induced cardiac death but not myocardial fibrosis in >21-m-old mdx mice, an end-stage model of Duchenne muscular dystrophy cardiomyopathy. *J. Mol. Cell Cardiol.*, **53**, 217–222.
35. Sandri, M., Minetti, C., Pedemonte, M. and Carraro, U. (1998) Apoptotic myonuclei in human Duchenne muscular dystrophy. *Lab Invest.*, **78**, 1005–1016.
36. Sandri, M., El Meslemani, A.H., Sandri, C., Schjerling, P., Vissing, K., Andersen, J.L., Rossini, K., Carraro, U. and Angelini, C. (2001) Caspase 3 expression correlates with skeletal muscle apoptosis in Duchenne and facioscapulo human muscular dystrophy. A potential target for pharmacological treatment? *J. Neuropathol. Exp. Neurol.*, **60**, 302–312.
37. Semenza, G.L. (2005) New insights into nNOS regulation of vascular homeostasis. *J. Clin. Invest.*, **115**, 2976–2978.
38. Huber-Abel, F.A., Gerber, M., Hoppeler, H. and Baum, O. (2012) Exercise-induced angiogenesis correlates with the up-regulated expression of neuronal nitric oxide synthase (nNOS) in human skeletal muscle. *Eur. J. Appl. Physiol.*, **112**, 155–162.
39. MacLennan, D.H. and Kranias, E.G. (2003) Phospholamban: a crucial regulator of cardiac contractility. *Nat. Rev. Mol. Cell. Biol.*, **4**, 566–577.
40. Turner, P.R., Westwood, T., Regen, C.M. and Steinhardt, R.A. (1988) Increased protein degradation results from elevated free calcium levels found in muscle from mdx mice. *Nature*, **335**, 735–738.
41. Zhang, Y.H., Zhang, M.H., Sears, C.E., Emanuel, K., Redwood, C., El-Armouche, A., Kranias, E.G. and Casadei, B. (2008) Reduced phospholamban phosphorylation is associated with impaired relaxation in left ventricular myocytes from neuronal NO synthase-deficient mice. *Circ. Res.*, **102**, 242–249.
42. Tsang, A., Hausenloy, D.J., Mocanu, M.M. and Yellon, D.M. (2004) Postconditioning: a form of "modified reperfusion" protects the myocardium by activating the phosphatidylinositol 3-kinase-Akt pathway. *Circ. Res.*, **95**, 230–232.
43. Pons, S., Martin, V., Portal, L., Zini, R., Morin, D., Berdeaux, A. and Ghaleb, B. (2013) Regular treadmill exercise restores cardioprotective signaling pathways in obese mice independently from improvement in associated co-morbidities. *J. Mol. Cell Cardiol.*, **54**, 82–89.
44. Kawasome, H., Papst, P., Webb, S., Keller, G.M., Johnson, G.L., Gelfand, E.W. and Terada, N. (1998) Targeted disruption of p70(s6k) defines its role in protein synthesis and rapamycin sensitivity. *Proc. Natl. Acad. Sci. USA*, **95**, 5033–5038.
45. McMullen, J.R., Shioi, T., Zhang, L., Tarnavski, O., Sherwood, M.C., Dorfman, A.L., Longnus, S., Pende, M., Martin, K.A., Blenis, J., Thomas, G. and Izumo, S. (2004) Deletion of ribosomal S6 kinases does not attenuate pathological, physiological, or insulin-like growth factor 1 receptor-phosphoinositide 3-kinase-induced cardiac hypertrophy. *Mol. Cell. Biol.*, **24**, 6231–6240.
46. Fingar, D.C., Salama, S., Tsou, C., Harlow, E. and Blenis, J. (2002) Mammalian cell size is controlled by mTOR and its downstream targets S6K1 and 4EBP1/eIF4E. *Genes Dev.*, **16**, 1472–1487.
47. Pende, M., Um, S.H., Mieulet, V., Sticker, M., Goss, V.L., Mestan, J., Mueller, M., Fumagalli, S., Kozma, S.C. and Thomas, G. (2004) S6K1(-/-)/S6K2(-/-) mice exhibit perinatal lethality and rapamycin-sensitive 5′-terminal oligopyrimidine mRNA translation and reveal a mitogen-activated protein kinase-dependent S6 kinase pathway. *Mol. Cell. Biol.*, **24**, 3112–3124.
48. Shin, J.H., Pan, X., Hakim, C.H., Yang, H.T., Yue, Y., Zhang, K., Terjung, R.L. and Duan, D. (2013) Microdystrophin ameliorates muscular dystrophy in the Canine model of Duchenne muscular dystrophy. *Mol. Ther.*, **21**, 750–757.
49. Bostick, B., Yue, Y., Lai, Y., Long, C., Li, D. and Duan, D. (2008) Adeno-associated virus serotype-9 microdystrophin gene therapy ameliorates electrocardiographic abnormalities in mdx mice. *Hum. Gene Ther.*, **19**, 851–856.

50. Yue, Y., Ghosh, A., Long, C., Bostick, B., Smith, B.F., Kornegay, J.N. and Duan, D. (2008) A single intravenous injection of adeno-associated virus serotype-9 leads to whole body skeletal muscle transduction in dogs. *Mol. Ther.*, **16**, 1944–1952.
51. Wolf, C.M., Moskowitz, I.P., Arno, S., Branco, D.M., Semsarian, C., Bernstein, S.A., Peterson, M., Maida, M., Morley, G.E., Fishman, G. *et al.* (2005) Somatic events modify hypertrophic cardiomyopathy pathology and link hypertrophy to arrhythmia. *Proc. Natl. Acad. Sci. USA*, **102**, 18123–18128.
52. Papadopulos, F., Spinelli, M., Valente, S., Foroni, L., Orrico, C., Alviano, F. and Pasquinelli, G. (2007) Common tasks in microscopic and ultrastructural image analysis using ImageJ. *Ultrastruct. Pathol.*, **31**, 401–407.
53. Xu, Z., Yue, Y., Lai, Y., Ye, C., Qiu, J., Pintel, D.J. and Duan, D. (2004) Trans-splicing adeno-associated viral vector-mediated gene therapy is limited by the accumulation of spliced mRNA but not by dual vector coinfection efficiency. *Hum. Gene Ther.*, **15**, 896–905.